BUILD SIMUL (2015) 8: 443 – 452
DOI 10.1007/s12273-015-0221-z

Estimation of indoor contamination source location by using variational continuous assimilation method

Tomohito Matsuo (✉), Akira Kondo, Hikari Shimadera, Takahiro Kyuno, Yoshio Inoue

Graduate School of Engineering, Osaka University, 2-1 Yamadaoka, Suita-shi, Osaka 565-0871, Japan

Research Article

Abstract

Information on concentration of contaminants is important for management of indoor air quality. Recently, data assimilation techniques are used in order to accurately estimate location and intensity of contamination source in addition to concentration field. In this study, the variational continuous assimilation (VCA) method, which was originally developed in meteorological simulations, was applied to estimates of indoor air quality. The method modifies the governing equations of computational fluid dynamics (CFD) model by adding a correction term which reduces the error between original CFD calculation and observed data. In the mass conservation equation, the correction term can be assumed to be a pseudo source term. The validity of VCA method was confirmed by numerical experiments for two-dimensional steady-state calculation with the following procedures: (i) "true" concentration field was produced by CFD calculations with "true" concentration source; (ii) "pseudo-observation" data were extracted from "true" concentration field; (iii) the VCA method was applied to "false" CFD calculations without contamination source to produce "corrected" concentration field using "pseudo-observation" data; (iv) "corrected" concentration field and contamination source were compared with "true" dataset. The numerical experiments revealed the following findings: the VCA method can identify the area where the contamination source was located; and the VCA method can also reduce errors between "true" and CFD-calculated concentration field although the peak concentration was not well-estimated. These results suggest that the VCA method is a utilizable method to estimate concentration field, and location and intensity of contamination source.

Keywords

VCA,
CFD,
indoor air quality,
data assimilation,
source identification,
steady calculation

Article History

Received: 25 December 2014
Revised: 18 February 2015
Accepted: 9 March 2015

Indoor/Outdoor Airflow and Air Quality

1 Introduction

Indoor contaminants such as airborne particles or disease agents induce adverse health effects. To assess, manage, and effectively decontaminate the contaminants, it is necessary to know the concentration field and source location of the contaminant. In order to estimate concentration field, there are typically two methods of measurements or computational fluid dynamics (CFD). However, some limitations exist for both methods. Measurements can obtain accurate information about concentration field, but these data are often spatially discrete. On the other hand, CFD can obtain information of entire field if the boundary conditions are accurately given. In many cases, however, boundary conditions such as the location and intensity of contamination source are not well known. To overcome these limitations, a data assimilation method can be used, which can correct CFD calculations by assimilating observed data.

Some assimilation methods modify the calculated values directly. A commonly used assimilation method is called the nudging method, in which CFD calculation is modified to be in good agreement with observations by a "nudging" term. The nudging method is easy to apply. However, it is difficult to select appropriate nudging coefficients because they have great impact on the results in addition to little physical meaning. There is a work which used a data assimilation method to determine the optimal nudging coefficients (Zou et al. 1992). Another typical assimilation method is the adjoint method (Le Dimet and Talagrand 1986). The adjoint method differs from other methods on the point that it corrects not for calculation values but for initial condition. The adjoint method uses an objective

E-mail: matsuo@ea.see.eng.osaka-u.ac.jp

function consisting of the sum of square errors, and corrects initial condition for minimizing the objective function. These methods, however, have some limitations. It was pointed out that if a model is imperfect, a correct initial condition will not achieve correct values because of the "model drift" from the attractor of nature induced by imperfection of the model (Toth and Peña 2007). Besides, it was found that if the "imperfect" model is used, the number of observation data required to obtain a good result with high probability will increase in comparison to the case that a "perfect" model is used (Kovalets et al. 2011). These results suggest that if a model is imperfect, data assimilations should modify the model rather than the initial or boundary conditions. Some assimilation methods can avoid this problem by reducing imperfection of a model. Kondo et al. (2010) used an objective function called cost function which consisted not only of the difference between observed and calculated values but also remainder of the governing equations. The calculated values are modified to minimize the cost function, so that they would be consistent with the observations and satisfy the governing equations. Alternatively, Derber (1989) modified the adjoint method and presented the variational continuous assimilation (VCA) method. Although the VCA method also used an objective function in the same way as the adjoint method, but the VCA method modifies not initial condition but a numerical model by introducing a correction term to the model equations. By employing these methods which intend to reduce imperfection of the model, aforementioned problems can be avoided. However it was pointed out that the "identifiability" of 4-D variational data assimilation methods was not always secured, and therefore the results should be tested further (Navon 1998).

There are some specialized assimilation methods to identify the source location and intensity. The quasi-reversibility (QR) method and the pseudo-reversibility (PR) method solve convection diffusion equation reversely to identify the location and the intensity of a contamination source (Zhang and Chen 2007a, b). The QR method solves the equations with a fourth-order stabilization term instead of a second-order diffusion term using the negative time step. The PR method, on the other hand, solves the equation without diffusion term using positive time step and reversed flow field. It was concluded that the QR method was slightly better than the PR method in terms of accuracy, but the QR method required more computational time. In addition, there are some methods to estimate the behavior of airborne particles. The behavior of airborne particles depends on several variables such as their radius. Chen et al. (2012) investigated the effect of near-wall heat source on particle deposition, and Tung et al. (2010) investigated the behavior of particles in industrial clean rooms with various particle radius and tool coverage. To estimate concentration of indoor airborne particles, Zhang et al. (2012) used the Lagrangian-reversibility method, which employed a reversed flow field, and showed that the method performed a little better than the PR method. Although Wang et al. (2013) developed an original method to identify an unknown point source in steady-state flow and concentration field, the method is only applicable to identification of single point source. The probability-based CFD modeling which uses the results of CFD calculation for all the potential point sources has the same limitation though the method could identify the source location with very high accuracy by using the limited number of sensor(s) (Liu and Zhai 2008). Assuming that the potential locations of source(s) are limited, rapid identification of the source location(s) can be performed by using the limited number of sensors (Cai et al. 2012, 2014). These studies indicate that the accuracy of source estimation can be improved by imposing a restriction about the source information. If the objective building is large and complicated, the method of probability-based inverse multi-zone modeling can be applied effectively, in order to identify the zone in which the contaminant source is located (Liu and Zhai 2009). The method uses multi-zone model created by simplification of the objective building consisting of several rooms, supply and return air terminals, etc., and calculates the transportation between each zone. The method cannot identify the exact location of the source though it can identify the zone including the source rapidly and effectively.

In this study, the VCA method was employed, and was modified in order to identify the source location and intensity. There are several reasons why the VCA method was used. First, the VCA method can explain the physical meaning of its correction term, which is assumed to be the source term in the contamination source estimation, as described in Section 2.2. Second, the method does not require any assumptions about the number and the form of the contamination source(s), so that the method can be used for source estimation for not only single point source, but also nonpoint source(s). In addition, though the VCA method was used only for identification of contamination source location and intensity in this study, the method can be used to correct the model imperfection at least in principle. In other words, the VCA method was chosen because of its versatility and expansibility for the future study.

2 Application of the VCA method for source estimation

2.1 Governing equations of the VCA method

The VCA method can be divided into two parts: the CFD calculation and the VCA calculation. In the CFD calculation, flow, thermal and concentration fields are calculated by CFD model whose governing equation can be given by

$$\boldsymbol{\Psi}^n = \boldsymbol{A}^n\boldsymbol{\Psi}^{n-1} + \boldsymbol{\lambda}^n\boldsymbol{\phi} \tag{1}$$

where $\boldsymbol{\Psi}^n$ is the vector consisted of calculated values at n-th time step t^n, and $\boldsymbol{A}^n$ is a non-linear operator acting upon $\boldsymbol{\Psi}^{n-1}$. The correction term $\boldsymbol{\lambda}^n\boldsymbol{\phi}$ consists of a prespecified time-dependent variable $\boldsymbol{\lambda}^n$ and a space-dependent vector $\boldsymbol{\phi}$. The variable $\boldsymbol{\lambda}^n$ is used to control the distribution of a correction vector over the assimilation interval. The VCA method corrects calculations by optimizing the correction vector $\boldsymbol{\phi}$.

In the VCA calculation, the objective function is defined as the difference between calculated and observed values, and is given by

$$I = \frac{1}{2}\sum_{p=1}^{P}\left(\boldsymbol{\Psi}^p - \tilde{\boldsymbol{\Psi}}^p\right)^{\mathrm{T}}\left(\boldsymbol{\Psi}^p - \tilde{\boldsymbol{\Psi}}^p\right) \tag{2}$$

where $\boldsymbol{\Psi}^p$ is the calculated vector of the p-th time step, and tilde denotes observation. P is the number of observation. Further, the $(\ )^{\mathrm{T}}$ notation denotes the transpose of a vector or a matrix.

The VCA method modifies the correction vector using the gradient of the objective function with respect to the correction vector. The gradient is given by

$$\frac{\partial I}{\partial \boldsymbol{\phi}} = \sum_{p=1}^{P}\left(\frac{\partial \boldsymbol{\Psi}^p}{\partial \boldsymbol{\phi}}\right)^{\mathrm{T}}\left(\boldsymbol{\Psi}^p - \tilde{\boldsymbol{\Psi}}^p\right) \tag{3}$$

By the steepest descent method given by Eq. (4), the VCA method obtains the optimal correction vector which minimizes the objective function.

$$\boldsymbol{\phi}^{k+1} = \boldsymbol{\phi}^k + \alpha\left.\frac{\partial I}{\partial \boldsymbol{\phi}}\right|_{\phi=\phi^k} \tag{4}$$

The more details of the VCA method are described in the previous work (Derber 1989).

2.2 Technique to estimate contamination source by the VCA method

In ordinal application of the VCA method, the correction term $\boldsymbol{\lambda}^n\boldsymbol{\phi}$ is used to modify the CFD calculation to minimize the difference between observed and calculated values. In this study, however, the correction term $\boldsymbol{\lambda}^n\boldsymbol{\phi}$ was also used for source estimation. In this section, the methodology of source estimation is described.

When the correct flow field and initial conditions are assumed to be known as the previous works (Zhang and Chen 2007a, b; Zhang et al. 2012; Kato et al. 2002, 2004; Neupauer and Wilson 2005; Keats et al. 2007), the convection and diffusion of contaminants can be accurately calculated by CFD; the difference between calculated and observed values is caused only by the source term $\boldsymbol{S}$. Under the assumption, the correction term $\boldsymbol{\lambda}^n\boldsymbol{\phi}$ can be converted to the source term by Eq. (5) to Eq. (9).

First, the mass conservation equation is given by

$$\frac{\partial \boldsymbol{C}}{\partial t} + \nabla\cdot(\boldsymbol{v}\boldsymbol{C}) = \nabla\cdot(\Gamma\nabla\boldsymbol{C}) + \boldsymbol{S} \tag{5}$$

where $\boldsymbol{C}$ is the contaminant concentration, $\boldsymbol{v}$ is the velocity vector, Γ is the coefficient of diffusion. The $\nabla\cdot$ notation denotes the divergence, and the ∇ notation denotes the gradient. $\boldsymbol{S}$ is the source intensity, which is assumed as a constant variable.

By using non-linear operator $\boldsymbol{A}^{n+1}$ acting upon $\boldsymbol{C}^n$, Eq. (5) can be discretized as

$$\boldsymbol{C}^{n+1} = \boldsymbol{A}^{n+1}\boldsymbol{C}^n + \boldsymbol{A}^{n+1}\boldsymbol{S}^* \tag{6}$$

where $\boldsymbol{S}^*$ is expressed as $\boldsymbol{S}^* = \boldsymbol{S}\cdot\Delta t$ and Δt denotes the time between n-th and $(n+1)$-th calculation steps.

By adding correction term into Eq. (6), Eq. (7) is given by

$$\boldsymbol{C}^{n+1} = \boldsymbol{A}^{n+1}\boldsymbol{C}^n + \boldsymbol{A}^{n+1}\boldsymbol{S}^* + \boldsymbol{\lambda}^{n+1}\boldsymbol{\phi} \tag{7}$$

As mentioned above, the difference between calculated and observed values is caused only by source term. If the correct and incorrect source terms are expressed by $\boldsymbol{S}^*_{\text{true}}$ and $\boldsymbol{S}^*_{\text{false}}$, respectively, the following equation is obtained:

$$\boldsymbol{A}^{n+1}\boldsymbol{S}^*_{\text{true}} + \boldsymbol{\lambda}^n\boldsymbol{\phi}\big|_{S^*=S^*_{\text{true}}} = \boldsymbol{A}^{n+1}\boldsymbol{S}^*_{\text{false}} + \boldsymbol{\lambda}^n\boldsymbol{\phi}\big|_{S^*=S^*_{\text{false}}} \tag{8}$$

where $\boldsymbol{\lambda}^n\boldsymbol{\phi}$ is the function of $\boldsymbol{S}^*$; when $\boldsymbol{S}^*$ is correct, $\boldsymbol{\lambda}^n\boldsymbol{\phi}$ is zero because there is no need to correct. When $\boldsymbol{S}^*_{\text{false}}$ is zero, the expression of Eq. (8) is given by

$$\boldsymbol{A}^{n+1}\boldsymbol{S}^*_{\text{true}} = \boldsymbol{\lambda}^n\boldsymbol{\phi}\big|_{S^*=0} \tag{9}$$

Therefore, assuming that the source term $\boldsymbol{S}^*$ is zero in calculation, the correction term $\boldsymbol{\lambda}^n\boldsymbol{\phi}$ will become equivalent to the effect of true source term. According to this, the distribution of correction vector was assumed as the estimated source location and intensity in the numerical experiments.

As mentioned in Section 2.1, the time-dependent matrix $\boldsymbol{\lambda}^n$ has to be prespecified. This means that the time variation of the emission from the contamination source should be known because the value of $\boldsymbol{\lambda}^n$ depends on the emission in the source estimation. Assuming that the source intensity is constant, $\boldsymbol{\lambda}^n$ is the identity matrix for the n-th time step in which the emission is occurring, and zero matrix for the others. When the constant emission is assumed, especially, all the $\boldsymbol{\lambda}$'s are identity matrixes.

Figure 1 shows the flowchart procedure for the VCA application in the current study.

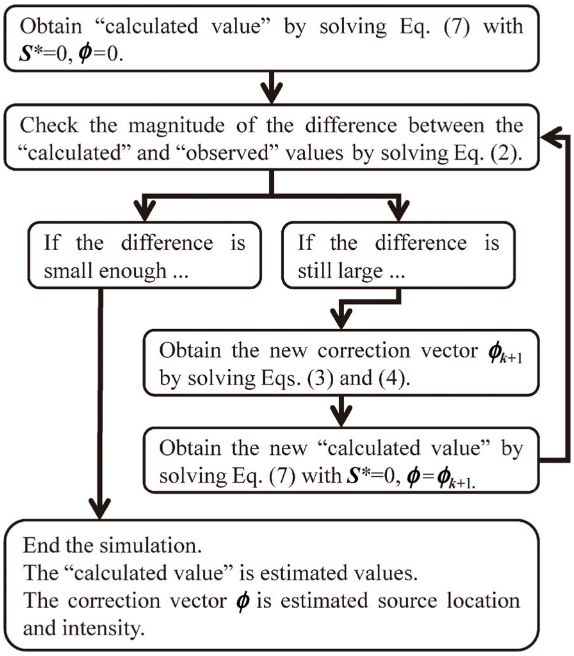

Fig. 1 Flowchart of the VCA method for identification of the contamination source and estimation of concentration of the contamination in this study

3 Numerical experiments of source estimation with the VCA method

3.1 Objective room

In order to confirm the validity of the VCA method for indoor contamination source estimation, the VCA method was applied to the model of a simple two-dimensional field. For simplification, the steady-state flow and concentration fields were assumed in the numerical experiments, though the VCA method was originally developed to be applied to both of steady and unsteady process (Derber 1989).

In this study, 33 cases of numerical experiments were performed for each contamination source shown in Fig. 2. The boundary conditions are displayed in Table 1. It was

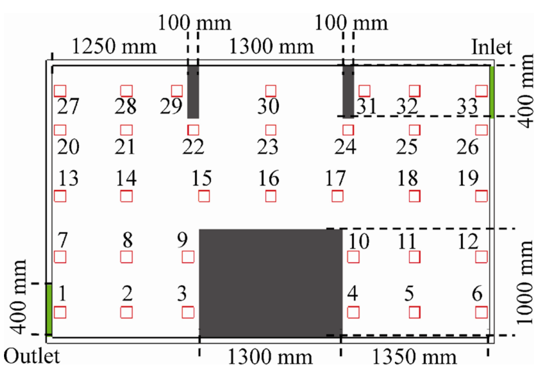

Fig. 2 Objective room with the locations of the contamination source for the 33 cases of the numerical experiments

Table 1 Information on objective room and boundary conditions

Room Size	4.0 m × 2.5 m
Mesh	Size: 0.05 m × 0.05 m (uniform) Number: 80 × 50
Inlet	0.4 $m \cdot s^{-1}$ (uniform)
Outlet	Free boundary
Contamination source	Size: 0.1 m × 0.1 m Intensity: 4.0 $g \cdot m^{-3} \cdot s^{-1}$(constant)

assumed that the objective room had unit length for depth direction so that the units [$g \cdot m^{-3} \cdot s^{-1}$] and [$g \cdot m^{-3}$] were used for source intensity and concentration, respectively.

3.2 Discretization of the governing equations

In the numerical experiments, the flow and concentration fields were assumed to be steady-state condition, which means $\boldsymbol{\lambda}^n$ is independent from time and is always identity matrix.

For the numerical experiments, the simulation tool of our own composition was used because of the requirement to add the function to perform the VCA calculation. The governing equations of CFD calculation are momentum equation, continuity equation, and mass conservation equation. These equations were discretized by finite volume method. The SIMPLE method was used for the iterative solving of flow and pressure fields (Patankar 1980). Besides, the method used the standard k–epsilon model for turbulence model, the first-order Euler method for the differencing time, the power-low scheme for differencing convection and diffusion.

The grid independency was checked by comparing the CFD calculation result of the grid with that of twice finer grid, and almost same results were obtained. The reliability of our tool was also validated by comparing the result of our tool with that of OpenFOAM (data not shown).

In this study, only the concentration field was corrected by the VCA method, so that the operator $\boldsymbol{A}^n$ was obtained from only the mass conservation equation.

3.3 Location of observation points

The positions of observed data should be decided carefully because it has a great impact on the result of assimilation. Our previous study indicated that observation points should be located according to following criteria: (i) they should be located under the lee of the contamination source, (ii) they should be located on the same streamline with contamination source (Matsuo et al. 2014). Thus the observation points were settled to satisfy these criteria. The streamline and observation points are shown in Fig. 3(a). According to the streamline pattern, the objective room

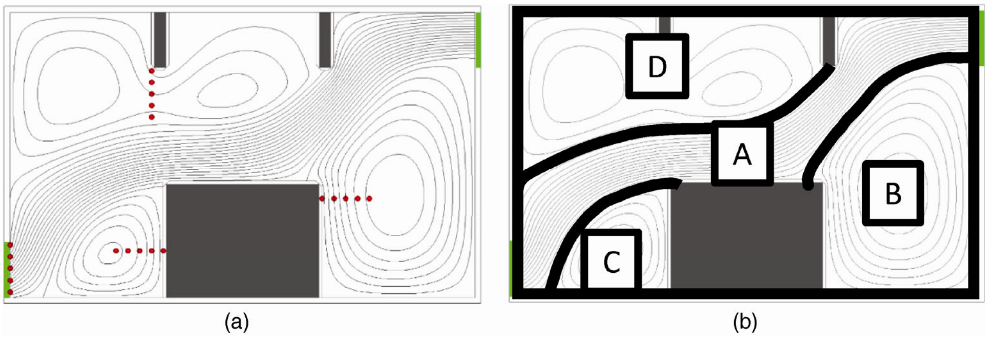

Fig. 3 (a) Observation points (red dots), (b) divided areas for the first numerical experiment according to the streamline pattern (black line)

was divided into four areas of one mainstream from inlet to outlet (area A), and three large eddies located right-hand side of the room (area B), lower left-hand side (area C), and upper side including two small eddies (area D) as shown in Fig. 3(b). For each area, the observation points should be settled to satisfy the aforementioned criteria, as shown in Fig. 3(a). In area A, observation points were settled at outlet, because the outlet was located at the most leeward in the flow. In the areas B, C, and D, observation points only had to be located in the eddy because the contaminants would circulate according to the eddy.

In addition, the number of observation points is also important from the view of the cost. Because the VCA method requires a few observed points which detect the contaminant in order to estimate the source location accurately, 5 sensors for each area were located so that a few sensors could detect the contaminant wherever the contamination source was located.

As mentioned above, the distribution of correction vector means the location and intensity of the contamination source, so when the peak correction vector is located in area A, the estimated contamination source is also located in area A. If the estimated contamination source is located in the same area with the "true" source, the source location is assumed to be "well-identified".

3.4 Creating "pseudo-observed data" and "calculated values"

In the numerical experiments, "pseudo-observed data" was created by CFD calculation as followed. The "true" values were created by the CFD calculation with the "true" boundary conditions (which shown in Table 1); and then, some values were extracted from "true" values and assumed to be the "pseudo-observed data". In the "pseudo-observed data", no observation error was assumed.

On the other hand, a CFD calculation carried out with no information of contamination source was assumed as "calculated values" for the application of the VCA method. In this CFD calculation, the source term $\boldsymbol{S}^*$ was assumed to be zero.

The VCA method was applied to "calculated values" in order to reconcile the difference between the "calculated values" and the "pseudo-observed data".

3.5 Strategy for identification

As Navon (1998) pointed out that the result of a 4-D variational data assimilation was not always secured the uniqueness, it is difficult to perform source estimation with a high degree of accuracy. To overcome this problem, we employed the iteration strategy as follows: (i) the objective room was divided into several areas according to the streamline pattern; (ii) the observation points were settled for each area to satisfy the aforementioned conditions; (iii) the area including contamination source was identified by the application of the VCA method; (iv) the locations of observation points were modified to subdivide the identified area into several more fine areas according to the streamline pattern as shown in Fig. 4.

This process can be applied repeatedly till the source location is identified accurately enough. In this study, the numerical experiments were performed twice. In the first numerical experiment, the objective room was divided into four areas as shown in Fig. 3(b) with the observation points shown in Fig. 3(a). When it had been estimated that the contamination source had been located in area A (case A), the area was subdivided into areas A1, A2, and A3 as shown in Fig. 4(e), and then the second numerical experiment were performed with the observation points shown in Fig. 4(a). In the same way, when it had been estimated that the source were located in areas B, C or D (cases B, C, and D, respectively), the area were subdivided as shown in Figs. 4(b), (c), and (d), respectively, and then the second numerical experiment were performed with the observation points shown in Figs. 4(f), (g), and (h), respectively.

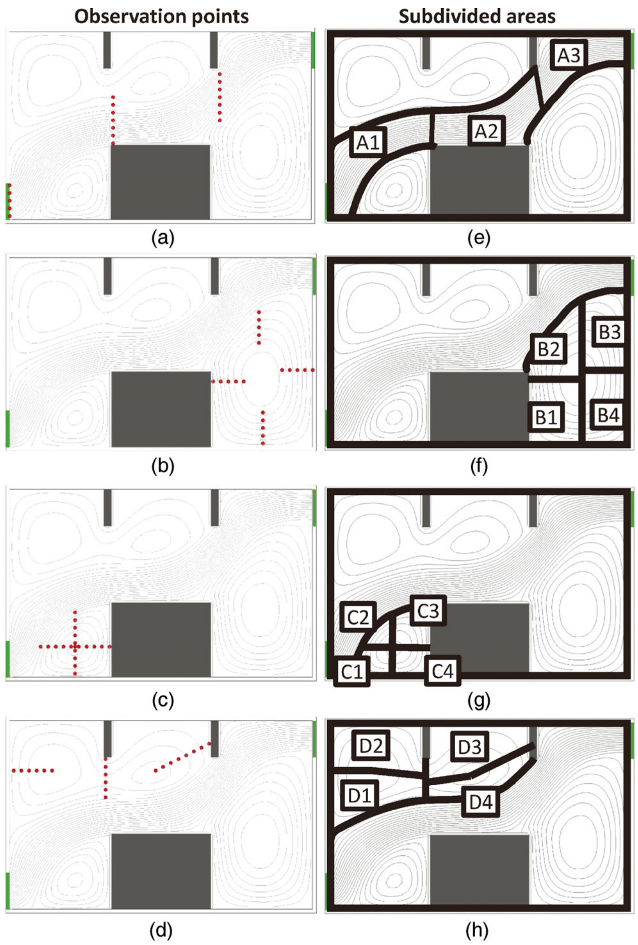

Fig. 4 Observation points of cases (a) A, (b) B, (c) C, and (d) D; and subdivided areas according to the streamline pattern for the second numerical experiment of cases (e) A, (f) B, (g) C, and (h) D

In the second numerical experiment, the source location was assumed to be "well-identified" when the estimated source location (the peak correction vector) was located in the same subdivided area with the "true" source.

4 Results and discussion

4.1 Results of the first numerical experiment

Figures 5(a), (b), (c), and (d) show the "true" and "corrected" concentration fields of source Nos. 2, 12, 16 and 20, respectively. The VCA method could estimate the concentration field roughly, but it could not catch the peak concentrations. Figures 5(e), (f), (g), and (h) show that the distributions of correction vector (estimated source location and intensity) with source Nos. 2, 12, 16 and 20, respectively. The peak correction vectors tend to distribute near the observation points which located in the same streamline with contamination source. Thus, even if the location of contamination source is unknown, the VCA method can identify the area in which the contamination source located. Figure 5(e) shows that the peak correction vector is located near the observation points of area C. Figures 5(f), (g), and (h), in the same way, show that the peak correction vectors are located in area B, A, and D, respectively. These peaks are located in the same area with the "true" sources, so that these source locations of source Nos. 2, 12, 16, and 20 were "well-identified". Meanwhile, the peak intensities are much less than the "true" intensity, 4.0 $\mathrm{g{\cdot}m^{-3}{\cdot}s^{-1}}$. It is because that the value of correction vector is widely spread. In the case of source No. 2 (Fig. 5(e)), for example, there are more than 100 cells whose values of the correction vector were greater than $0.50 \times 10^{-2}\ \mathrm{g{\cdot}m^{-3}{\cdot}s^{-1}}$ though the size of "true" source is only 4 cells, and the sum of the correction vector value of all cells was almost the same with the correct value, 4.0.

All the results are summarized in Fig. 6. The contamination sources shown by the filled square mean that they were "well-identified". In 27 cases out of the 33 cases (82%), the VCA method could identify which divided area includes the contamination source, areas A, B, C, or D. However, in cases of source Nos. 9, 17, 24, 31, 32 and 33, the identifications of the area which includes the contamination source were failed.

These results indicate that it is difficult to identify the location of contamination source when the source is located at the edge of the areas divided according to the streamline pattern (source No. 9) or/and located far from the observation points in which located the same streamline with the source (source Nos. 17, 24, 31, 32 and 33).

In addition, because the correction vectors were distributed according to the flow field, it is obvious that the estimation results heavily depend on the flow field. This means that the errors of estimation would increase in practice because the errors of flow field inevitably exist, though the flow field was assumed to have no error in the present numerical experiments.

4.2 Validity of concentration field estimation

In order to validate the concentration field corrected by the VCA method, Root-mean-square error (RMSE) of concentration between "true" and "corrected" values were used. The RMSE value $E_{\text{corrected}}$ is given by

$$E_{\text{corrected}} = \sqrt{\frac{1}{M_{\text{all}}}\sum_{l=1}^{M_{\text{all}}}\left(C_{l,\text{true}} - C_{l,\text{corrected}}\right)^2} \tag{10}$$

where M_{all} is the number of calculation cells, $C_{l,\text{true}}$ and $C_{l,\text{corrected}}$ are the "true" and "corrected" concentration at the l-th cell, respectively.

In order to clarify the reduction rate of the error, the RMSE for corrected values $E_{\text{corrected}}$ was normalized by the

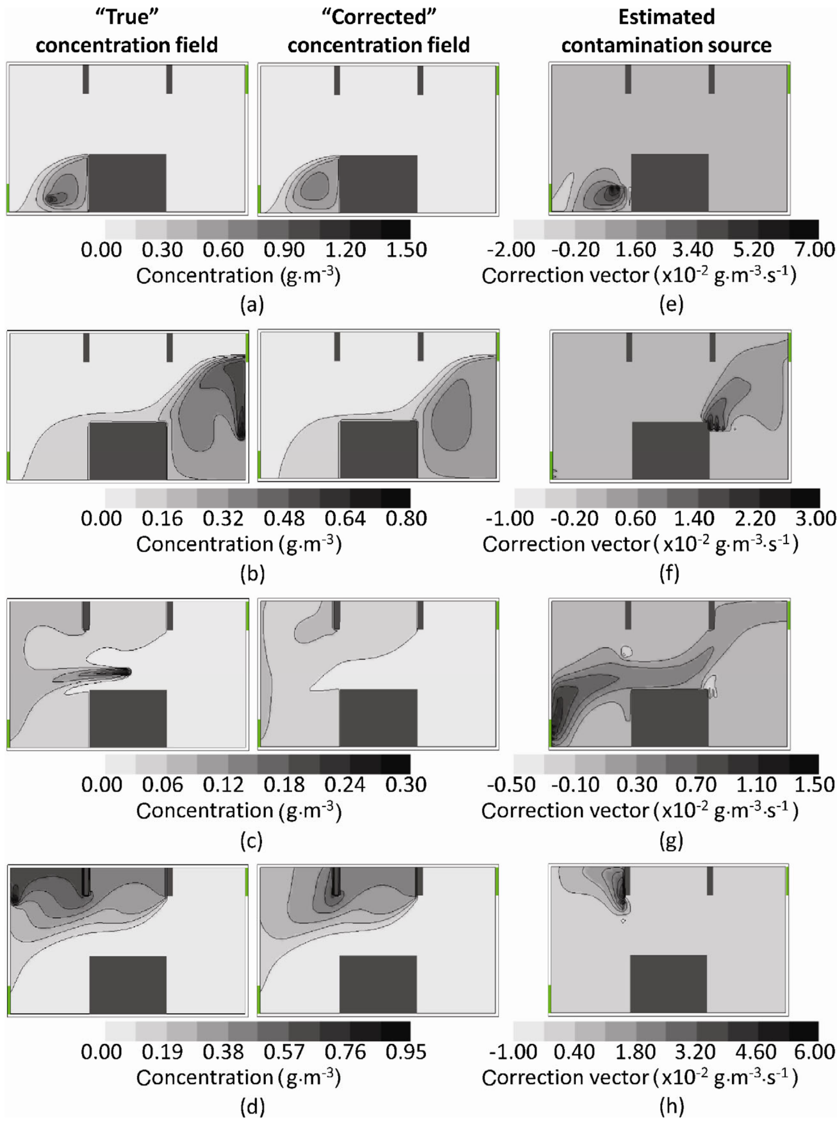

Fig. 5 "True" and "corrected" concentration fields of the first numerical experiment for the sources (a) No. 2, (b) No. 12, (c) No. 16, and (d) No. 20; and distributions of correction vector (estimated contamination source location and intensity) of the first numerical experiment for the sources (e) No. 2, (f) No. 12, (g) No. 16, and (h) No. 20

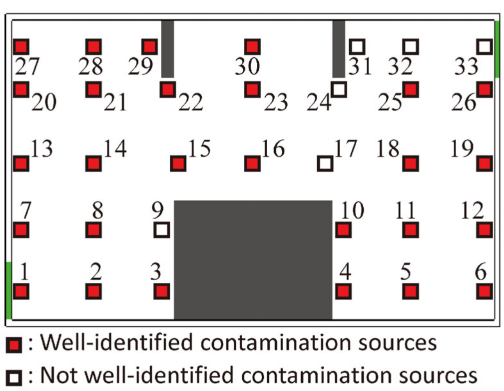

Fig. 6 Locations of the contamination source whose location was well-identified by the VCA method in the first numerical experiment

RMSE value for uncorrected values $E_{\mathrm{calculated}}$. The normalized RMSE E_{normal} is given by

$$E_{\mathrm{normal}} = \frac{E_{\mathrm{corrected}}}{E_{\mathrm{calculated}}} \tag{11}$$

Figure 7 shows the histogram of the normalized RMSEs in the first experiment. In most cases, the VCA reduced the error. However, the normalized RMSEs were increased in the two cases of source Nos. 1 and 7, whose "true" and "corrected" concentrations and the distributions of correction vector are shown in Fig. 8. In these two cases, the error sensitivity was relatively high because the amount of "true" concentration was quite small. The corrected concentration field was overestimated in windward. These results indicate

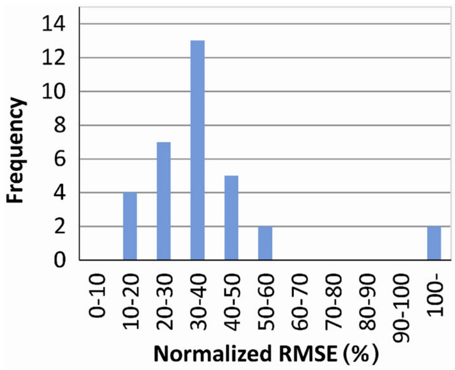

Fig. 7 Histogram of the normalized RMSEs for the first numerical experiment

that it is difficult to estimate the concentration of contamination when the contamination source is located near the outlet.

As a result, in 31 out of the 33 cases (94%), the normalized RMSEs of concentration were less than 60%. The normalized RMSEs for source Nos. 9, 17, 24, 31, 32 and 33, for which the identifications of contamination source location were failed, were also decreased. This result indicates that the VCA method can estimate concentration field more accurately than the case of only CFD.

4.3 The modification of locations of observation points

By the first numerical experiment of the VCA method, the area including the contamination source might be identified. In order to subdivide the area, The VCA method can be applied repeatedly with modified observation points. Corresponding to each area shown in Fig. 3(b), the locations of observation points were modified as shown in Fig. 4. According to the results of the first identification of the area, the areas were subdivided into more fine areas. The area A, for example, was subdivided into area A1 to A3. The area B to D, in the same way, were subdivided into area B1 to B4, area C1 to C4, and area D1 to D4.

In the second numerical experiment, the source location was assumed to be "well-identified" only when the estimated source location (the peak correction vector) was located in the same subdivided area as shown in Fig. 4 with the "true" source.

4.4 Results of the second numerical experiment

According to the results of the second numerical experiment of the VCA method, the sources "well-identified" in the first numerical experiment were also "well-identified" in the second numerical experiment by the VCA method. This result means that the source location can be identified more specifically by applying the VCA method repeatedly. Figure 9 shows the histogram of normalized RMSEs of "corrected" concentration field of the second numerical experiment. The accuracy of estimation of concentration field can be improved by applying the VCA method repeatedly.

In the first and the second numerical experiments, the same number of the observation points were used, which suggests that the accuracy of the estimation can be improved

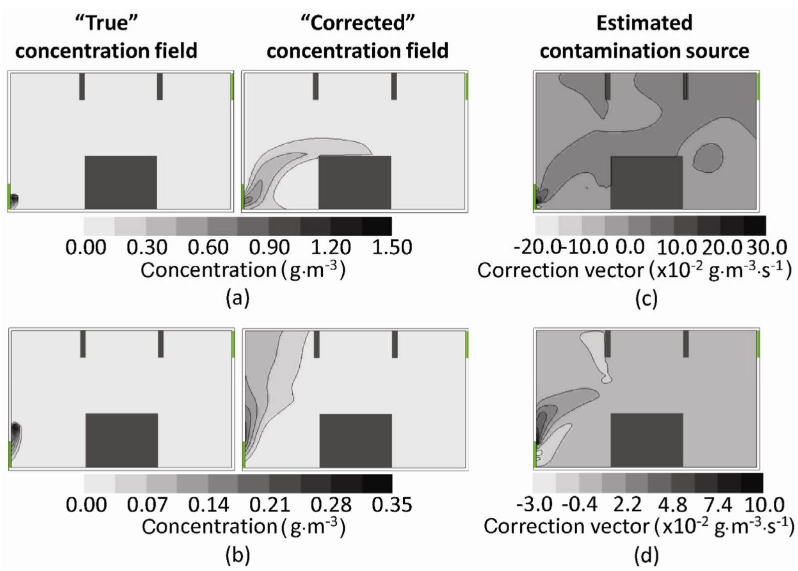

Fig. 8 "True" and "corrected" concentration fields of the first numerical experiment for the sources (a) No. 1 and (b) No. 7; and distributions of correction vector (estimated contamination source location and intensity) of the first numerical experiment for the sources (c) No. 1 and (d) No. 7

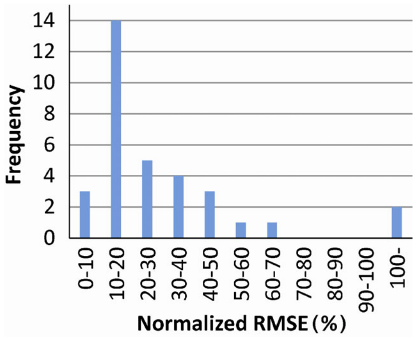

Fig. 9 Histogram of the normalized RMSEs for the second numerical experiment

by the location of the observation points. The number of the observation points, however, is also important to improve the accuracy of the estimation because the more observation points can be used, the finer areas the calculation domain can be divided into.

5 Conclusions

The VCA method was applied to estimate unknown concentration field and to identify unknown contamination source location and intensity, and was validated by the numerical experiments that were carried out for the two-dimensional steady state condition. In the experiments, it was assumed that the flow field was known and the observation data had no errors.

The numerical experiments revealed the following findings: (i) in 27 cases out of the 33 cases in the first numerical experiment, the VCA method could identify the area where the contamination source was located; (ii) the accuracy of identification of source location was decreased when the source was located at the edge of the areas divided according to the streamline pattern or far from observation points; (iii) when the identification of source location had succeeded in the first numerical experiment, the accuracy of identification was increased in the second experiment; (iv) in 31 cases out of the 33 cases in the first numerical experiment, the RMSEs of concentration fields of contamination were reduced although the peak concentrations were not well-estimated; (v) in the second experiment, the RMSEs were also reduced in most cases. These findings indicate that wherever the contamination source is located, the VCA method can identify the source location and intensity, and can estimate concentration field of contamination.

References

Chen X, Li A, Gao R (2012). Effects of near-wall heat source on particle deposition. *Building Simulation*, 5: 371–382.

Derber JC (1989). A variational continuous assimilation technique. *Monthly Weather Review*, 117: 2437–2446.

Cai H, Li X, Kong L, Ma X, Shao X (2012). Rapid identification of single constant source by considering characteristics of real sensors. *Journal of Central South University*, 19: 593–599.

Cai H, Li X, Chen Z, Wang M (2014). Rapid identification of multiple constantly-released contaminant sources in indoor environments with unknown release time. *Building and Environment*, 81: 7–19.

Kato S, Kajii Y, Itokazu R, Hirokawa J, Koda S, Kinjo Y (2004). Transport of atmospheric carbon monoxide, ozone, and hydrocarbons from Chinese coast to Okinawa island in the Western Pacific during winter. *Atmospheric Environment*, 38: 2975–2981.

Kato S, Pochanart P, Hirokawa J, Kajii Y, Akimoto H, Ozaki Y, Obi K, Katsuno T, Streets DG, Minko NP (2002). The influence of Siberian forest fires on carbon monoxide concentrations at Happo, Japan. *Atmospheric Environment*, 36: 385–390.

Keats A, Yee E, Lien FS (2007). Bayesian inference for source determination with applications to a complex urban environment. *Atmospheric Environment*, 41: 465–479.

Kondo A, Nakagawa H, Kaga A, Inoue Y (2010). Understanding of flow and scalar fields by combining measured data and CFD. *ASHRAE Transactions*, 116(2): 318–328.

Kovalets IV, Andronopoulos S, Venetsanos AG, Bartzis JG (2011). Identification of strength and location of stationary point source of atmospheric pollutant in urban conditions using computational fluid dynamics model. *Mathematics and Computers in Simulation*, 82: 244–257.

Le Dimet FX, Talagrand O (1986). Variational algorithms for analysis and assimilation of meteorological observations: theoretical aspects. *Tellus*, 38A: 97–110.

Liu X, Zhai Z (2008). Location identification for indoor instantaneous point contaminant source by probability-based inverse Computational Fluid Dynamics modeling. *Indoor Air*, 18: 2–11.

Liu X, Zhai ZJ (2009). Prompt tracking of indoor airborne contaminant source location with probability-based inverse multi-zone modeling. *Building and Environment*, 44: 1135–1143.

Matsuo T, Kondo A, Shimadera H, Inoue Y (2014). Source estimation of indoor contamination with variational continuous assimilation method. In: Proceedings of 25th International Symposium on Transport Phenomena (ISTP-25), Krabi, Thailand.

Navon IM (1998). Practical and theoretical aspects of adjoint parameter estimation and identifiability in meteorology and oceanography. *Dynamics of Atmospheres and Oceans*, 27: 55–79.

Neupauer RM, Wilson JL (2005). Backward probability model using multiple observations of contamination to identify groundwater contamination sources at the Massachusetts Military Reservation. *Water Resources Research*, 41(2): 1–14.

Patankar SV (1980). Numerical Heat Transfer and Fluid Flow. Washington, DC: Hemisphere Publishing Corporation.

Toth Z, Peña M (2007). Data assimilation and numerical forecasting with imperfect models: The mapping paradigm. *Physica D*, 230: 146–158.

Tung YC, Hu SC, Xu T, Wang RH (2010). Influence of ventilation arrangements on particle removal in industrial cleanrooms with various tool coverage. *Building Simulation*, 3: 3–13.

Wang X, Tao W, Lu Y, Wang F (2013). A method to identify the point source of indoor gaseous contaminant based on limited on-site steady concentration measurements. *Building Simulation*, 6: 395–402.

Zhang T, Chen Q (2007a). Identification of contaminant sources in enclosed environments by inverse CFD modeling. *Indoor Air*, 17: 167–177.

Zhang T, Chen Q (2007b). Identification of contaminant sources in enclosed spaces by a single sensor. *Indoor Air*, 17: 439–449.

Zhang T, Li H, Wang S (2012). Inversely tracking indoor airborne particles to locate their release sources. *Atmospheric Environment*, 55: 328–338.

Zou X, Navon IM, LeDemit FX (1992). An optimal nudging data assimilation scheme using parameter estimation. *Quarterly Journal of the Royal Meteorological Society*, 118: 1163–1186.